Acta Cryst C
STRUCTURAL CHEMISTRY

ISSN 2053-2296

Using cocrystals as a tool to study non-crystallizing molecules: crystal structure, Hirshfeld surface analysis and computational study of the 1:1 cocrystal of (*E*)-*N*-(3,4-difluorophenyl)-1-(pyridin-4-yl)methanimine and acetic acid

Addi Dana Sánchez-Pacheco,[a] Eduardo H. Huerta,[a] Josué Benjamín Espinosa-Camargo,[a,c] Evelyn Valeria Rodríguez-Nájera,[a] Diego Martínez-Otero,[b] Simón Hernández-Ortega[a] and Jesús Valdés-Martínez[a]*

[a]Instituto de Química, Universidad Nacional Autónoma de México, Circuito Exterior, Ciudad Universitaria, 04510 Coyoacán, Cd. Mx., Mexico, [b]CCIQS UAEM-UNAM, Universidad Nacional Autónoma de México, Carretera, Toluca-Atlacomulco Km. 14.5, Unidad San Cayetano, Toluca, 50200, Estado de México, Mexico, and [c]Tecnológico de Estudios Superiores de Ixtapaluca, Km 7 Carretera Ixtapaluca, Coatepec, CP 56580, Ixtapaluca, Estado de México, Mexico. *Correspondence e-mail: jvaldes@iquimica.unam.mx

Received 3 April 2024
Accepted 31 May 2024

Edited by R. Diniz, Universidade Federal de Minas Gerais, Brazil

Keywords: crystal structure; cocrystal; hydrogen bonding; π–π interactions; CrystalExplorer; AIM; NCI; methaninine; acetic acid.

CCDC reference: 2359735

Supporting information: this article has supporting information at journals.iucr.org/c

Using a 1:1 cocrystal of (*E*)-*N*-(3,4-difluorophenyl)-1-(pyridin-4-yl)methanimine with acetic acid, $C_{12}H_8F_2N_2{\cdot}C_2H_4O_2$, we investigate the influence of F atoms introduced to the aromatic ring on promoting π–π interactions. The cocrystal crystallizes in the triclinic space group $P1$. Through crystallographic analysis and computational studies, we reveal the molecular arrangement within this co-crystal, demonstrating the presence of hydrogen bonding between the acetic acid molecule and the pyridyl group, along with π–π interactions between the aromatic rings. Our findings highlight the importance of F atoms in promoting π–π interactions without necessitating full halogenation of the aromatic ring.

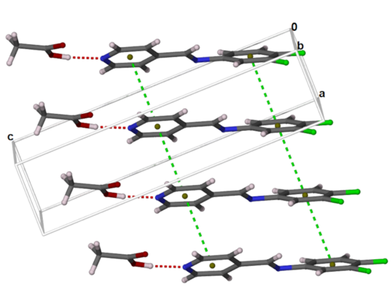

1. Introduction

Understanding intermolecular interactions is fundamental to designing and synthesizing functional solid-state materials. Although there are significant advances in our understanding, there is still much to comprehend (Brammer, 2017; Galek *et al.*, 2014; Gunawardana & Aakeröy, 2018). Our research investigates small molecules derived from Schiff bases having an aromatic ring (^{F}Ar) and a pyridyl group (py). These molecules can form three different types of intermolecular interactions: hydrogen bonds (H-bonds), interactions between the aromatic rings (π–π and C—H$\cdots\pi$) and halogen bonds (X-bonds) when F, Br or I atoms are present. We have introduced F atoms to the Ar ring (^{F}Ar) to increase the likelihood of π-interactions between the aromatic rings. We are looking to understand how the number and position of F atoms in ^{F}Ar affect the interactions and organization of the molecules in the crystal. Previous studies have indicated that the perfluorinated ^{F}Ar ring interacts with the py ring through π–π interactions in both Schiff base (Jaime-Adán *et al.*, 2024) and alkene analogue molecules [Cambridge Structural Database (CSD; Groom *et al.*, 2016) refcodes ADUJOA (Orbach *et al.*, 2012), EQOTOU (Mondal *et al.*, 2011), EQOTOU (Lucassen *et al.*, 2005) and RIDMOH (Aakeröy *et al.*, 2007)], while non-fluorinated or mono-fluorinated rings of the Schiff base and the analogue alkene only present C—H$\cdots\pi$ interactions. We aim to investigate how many F atoms are necessary to promote π–π interactions.

 https://doi.org/10.1107/S2053229624005187

Despite our best efforts, we were unable to crystallize disubstituted compounds successfully. However, we did manage to obtain a cocrystal of (*E*)-*N*-(3,4-difluorophenyl)-1-(pyridin-4-yl)methanimine (DFPPI) with acetic acid (AcOH), which is an acid that does not contain aromatic rings that may interfere with the possible aromatic interactions. In this article, we present the crystal structure of the 1:1 DFPPI–AcOH cocrystal, (**1**) (Scheme 1), and reveal the interactions that govern its stability through Hirshfeld surface analysis and computational methodologies.

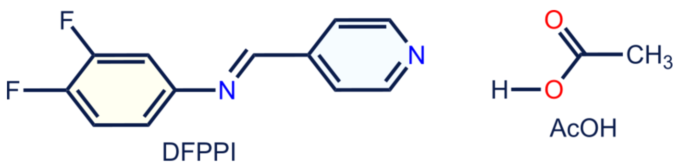

(**1**)

Scheme 1

2. Experimental

All solvents, starting materials and carboxylic acids were purchased from commercial sources and used without further purification. IR data were collected using a Nicolet 380 FT–IR instrument. The melting point (uncorrected) was determined using a Fischer–Johns Mel-Temp melting-point apparatus.

2.1. Synthesis and crystallization

DFPPI was obtained from an equimolar reaction of pyridine-4-carbaldehyde and 3,4-difluoroaniline as reported previously (Sánchez-Pacheco *et al.*, 2021). Crystals of (**1**) were obtained from a 9:1 (*v*/*v*) ethanol–acetic acid solution as a cream–yellow powder (m.p. 340–342 K). FT–IR (ATR) ν_{max}: 3058, 3030, 1627, 1597, 1107 cm^{-1}. ^{1}H NMR ($CDCl_3$, 300 MHz): δ 8.78 (*dd*, *J* = 6.0, 2.6 Hz, 2H), 8.43 (*s*, 1H), 7.74 (*dd*, *J* = 6.0, 2.7 Hz, 2H), 7.26–7.17 (*m*, 1H), 7.16–7.08 (*m*, 1H), 7.05–6.97 (*m*, 1H). DART+, *m*/*z*: 220, 219.

2.2. Refinement

Crystal data, data collection and structure refinement details are summarized in Table 1. Carbon-bound H atoms were placed in calculated positions and included in the refinement in the riding-model approximation, with U_{iso}(H) values set to 1.2U_{eq}(C). In the final analysis, we explored the isotropic displacement parameter refinement of the O and N atoms, but the results were not significant, so thermal anisotropy was applied. The oxygen-bound H atom was located from a difference Fourier map and refined with U_{iso}(H) = 1.5U_{eq}(O).

2.3. Computational studies

The analysis of electron density and interaction energies aims to discern the nature and strength of interactions within the cocrystal. The study began with calculating the Hirshfeld surface (Spackman *et al.*, 2021), where the d_{norm} and shape index (S) were then mapped to identify intermolecular interactions and detect π–π interactions, respectively. Afterward, pairwise interaction energies were computed to quantify interaction strength, and an energy framework was derived to characterize the stabilizing interactions within the network. Both the calculation of the Hirshfeld surface and the energy analysis were conducted in *CrystalExplorer*, employing the CE-B3LYP/6-31G(d,p) level with *TONTO* (Jayatilaka & Grimwood, 2003; Turner *et al.*, 2015; Mackenzie *et al.*, 2017). Further insights into the interactions were achieved through theoretical electron-density analysis using the GPUAM code (Cruz *et al.*, 2019; Hernández-Esparza *et al.*, 2014, 2018), which combines two methodologies, namely, the Quantum Theory of Atoms in Molecules (QTAIM) and the Non-Covalent Interactions (NCI) Index. The theoretical electron density was generated using *GAUSSIAN16* [B3LYP/6-31G(d,p)] (Frisch *et al.* 2016).

Table 1
Experimental details.

Crystal data	
Chemical formula	$C_{12}H_8F_2N_2{\cdot}C_2H_4O_2$
M_r	278.26
Crystal system, space group	Triclinic, $P\overline{1}$
Temperature (K)	100
a, *b*, *c* (Å)	3.8047 (1), 11.0101 (4), 15.4968 (6)
α, β, γ (°)	79.535 (1), 89.223 (1), 82.880 (1)
V (Å^3)	633.42 (4)
Z	2
Radiation type	Mo *Kα*
μ (mm^{-1})	0.12
Crystal size (mm)	0.35 × 0.28 × 0.21
Data collection	
Diffractometer	Bruker APEXII CCD
No. of measured, independent and observed [$I > 2\sigma(I)$] reflections	11642, 2896, 2531
R_{int}	0.083
$(\sin \theta/\lambda)_{max}$ (Å^{-1})	0.650
Refinement	
$R[F^2 > 2\sigma(F^2)]$, $wR(F^2)$, *S*	0.038, 0.110, 1.06
No. of reflections	2896
No. of parameters	185
No. of restraints	1
H-atom treatment	H atoms treated by a mixture of independent and constrained refinement
$\Delta\rho_{max}$, $\Delta\rho_{min}$ (e Å^{-3})	0.39, −0.28

Computer programs: *APEX2* (Bruker, 2005), *SAINT* (Bruker, 1998), *SHELXT* (Sheldrick, 2015*a*), *SHELXL* (Sheldrick, 2015*b*), *X-SEED 4* (Barbour, 2020), *CIFTAB* (Sheldrick, 2008) and *PLATON* (Spek, 2020).

3. Results and discussion

Cocrystal (**1**) consists of one DFPPI molecule and one acetic acid molecule in its asymmetric unit (Fig. 1). The crystal system is triclinic and belongs to the space group *P*1. The imine group has an *E* conformation. The DFPPI molecule is not planar, as evidenced by the relevant torsion angles (Table 2) and the dihedral angle of 29.89 (5)° between the planes of the pyridine (py) and aromatic (^{F}Ar) rings. The AcOH molecule shows C—O distances according to single and double C—O bonds, in agreement with the presence of an acid group and not a carboxylate, as expected for a cocrystal.

Table 2
Selected geometric parameters (Å, °).

O1—C14	1.3243 (14)	N2—C7	1.2739 (15)
O2—C14	1.2166 (14)	N2—C8	1.4188 (13)
C7—N2—C8	119.44 (9)	O2—C14—C15	123.74 (10)
N2—C7—C4	120.72 (10)	O1—C14—C15	112.80 (9)
O2—C14—O1	123.43 (10)		
C3—C4—C7—N2	−179.29 (10)	C7—N2—C8—C13	−151.63 (11)
C5—C4—C7—N2	0.01 (17)	C7—N2—C8—C9	30.40 (16)

Table 3
Hydrogen-bond geometry (Å, °).

D—H$\cdots A$	D—H	H$\cdots A$	$D\cdots A$	D—H$\cdots A$
O1—H1$\cdots$N1^{i}	0.86 (1)	1.83 (1)	2.6819 (12)	174 (2)
C2—H2$\cdots$O2^{ii}	0.95	2.64	3.3344 (14)	130
C3—H3$\cdots$O2^{iii}	0.95	2.48	3.3174 (14)	147
C9—H9$\cdots$O2^{iv}	0.95	2.56	3.5088 (14)	173
C13—H13$\cdots$O1^{v}	0.95	2.65	3.3713 (14)	134
C15—H15$B\cdots$F2^{vi}	0.98	2.61	3.5224 (14)	155

Symmetry codes: (i) $x+1, y, z$; (ii) $x-1, y, z$; (iii) $-x+1, -y+1, -z+1$; (iv) $-x+2, -y+1, -z+1$; (v) $-x+2, -y, -z+1$; (vi) $x-1, y, z+1$.

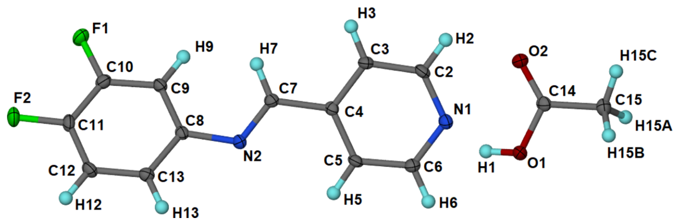

Figure 1
The asymmetric unit of cocrystal (**1**), showing the atom-numbering scheme. Displacement ellipsoids are drawn at the 50% probability level and H atoms at an arbitrary size.

The C—O bonds in the AcOH molecule are nearly in the same plane as the py ring. This is confirmed by the angle formed between the py ring and the heavy atoms of AcOH, which measures 10.80 (6)°.

The AcOH molecule forms an O1—H1$\cdots$N1^{i} hydrogen bond with the N1 atom of the py from the imine (Table 3). Moreover, it shows py$\cdots$py and ^{F}Ar$\cdots$^{F}Ar π–π interactions, with centroid–centroid distances of Cg(py)$\cdots$$Cg$(py) = 3.8047 (6) Å and Cg(^{F}Ar)$\cdots$$Cg$(^{F}Ar) = 3.8047 (7) Å; these interactions organize the molecules in columns [Fig. 2(*a*)] and the columns close pack to build the crystal [Fig. 2(*b*)].

We used the *CrystalExplorer* program to generate Hirshfield surfaces and mapped them with $d_{\rm norm}$ and shape index, and two-dimensional (2D) fingerprints to determine the intermolecular interactions (McKinnon *et al.*, 2007). Fig. 3 shows the 2D fingerprints of DFPPI and AcOH. The plots show the typical wing structures with a non-symmetric long pick, which corresponds to the N1$\cdots$H1 interaction on the DFPPI molecule and H1$\cdots$N1 in the AcOH molecule, corresponding to the O1—H1$\cdots$N1^{i} hydrogen bond between both molecules. There is another hydrogen bond, namely, C2—H2$\cdots$O2^{ii}, *i.e.* C2—H2$\cdots$O2 in DFPPI and O2$\cdots$H2—C2 in AcOH. Additionally, the fingerprint of DFPPI indicates bonds of the type C—H$\cdots$F and interactions between the C atoms, suggesting π–π interactions.

Fig. 4(*a*) displays the Hirshfeld surface, mapped with $d_{\rm norm}$, which shows the existence of O—H$\cdots$N(py) and C—H$\cdots$O hydrogen bonds. Fig. 4(*b*) shows the Hirshfeld surface mapped with shape index; the complementary blue and red triangles observed in the aromatic rings indicate the presence of π–π interactions between the ^{F}Ar and py rings (McKinnon *et al.*, 2004).

Table 4 presents selected results from the calculation of pairwise interaction energies relative to the DFPPI molecule, along with a colour-coded molecular cluster illustrating these interactions. As expected, the most robust interaction, highlighted in red, was observed between the DFPPI molecule and the AcOH molecule. This interaction involves a hydrogen bond between O—H(acid) and N(py), with a total interaction energy ($E_{\rm tot}$) of −49.4 kJ mol^{-1}. The interactions between DFPPI molecules stacked on top of each other, coloured in green in Table 4, follow in energy. According to the Hirshfeld

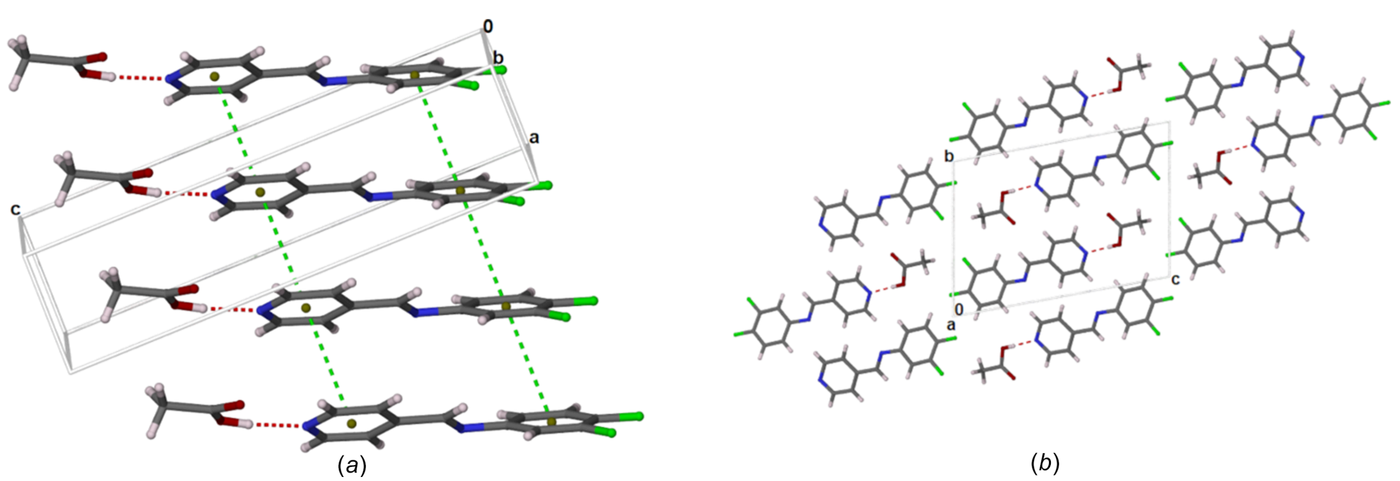

Figure 2
The intermolecular interactions in (**1**). Hydrogen bonds are indicated as red dashed lines and π–π interactions as green dashed lines. (*a*) View of the molecules organized in columns through π–π interactions. (*b*) The packing of molecules along the *a* axis, showing the O—H$\cdots$N(py) hydrogen bonding.

Table 4
Pairwise interaction energy analysis using B3LYP/6-311G(d,p) as the energy model.

The energies (E) are in kJ mol^{-1} and the radial distance (R) in Å. The colour-coded molecular cluster is related to the specific interaction energy.

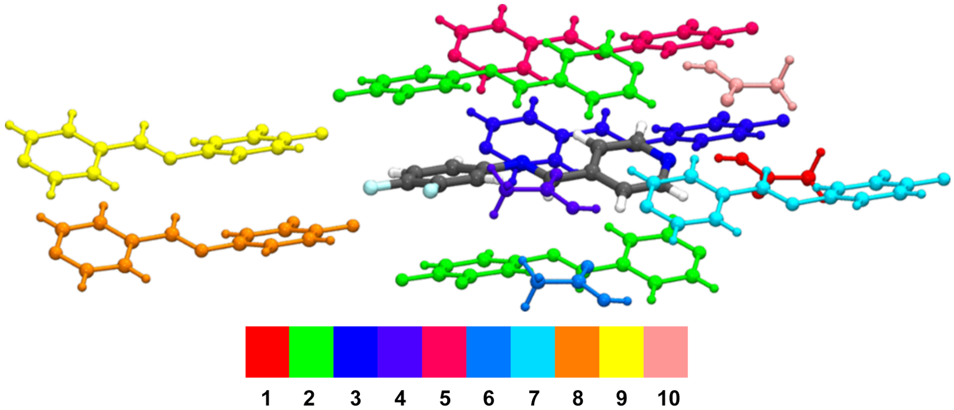

	No.	Symop	R	E_{ele}	E_{pol}	E_{dis}	E_{rep}	E_{tot}	E	E_{BSSE}
1	1	–	8.79	−81.5	−18.8	−11.5	98.2	−49.4	−53.9	−41.8
2	2	x, y, z	3.80	0.3	−1.1	−59.0	32.0	−32.1	−51.5	−33.6
3	1	$-x, -y, -z$	7.90	−9.9	−1.1	−24.5	18.1	−21.4	−34.6	−24.3
4	1	–	4.76	−12.3	−3.3	−12.2	11.2	−19.2	30.7	−20.7
5	1	$-x, -y, -z$	7.22	−9.1	−1.3	−24.1	22.4	−17.7	−31.2	−23.6
6	1	–	5.08	−9.1	−1.3	−24.1	22.4	−17.7	−31.2	−23.6
7	1	$-x, -y, -z$	10.07	−4.4	−0.9	−14.2	13.0	−9.7	−15.6	−11.4
8	1	$-x, -y, -z$	10.81	−4.0	−0.5	−8.8	5.2	−9.0	−19.1	10.6
9	1	$-x, -y, -z$	11.57	−3.4	−0.4	−7.3	3.0	−8.4	−17.11	−9.54
10	1	–	8.14	−2.0	−0.6	−5.1	0.9	−6.4	−9.9	−6.7
Scale factors for benchmarked energy model										
Energy model				k_{ele}	k_{pol}	k_{dis}	k_{rep}			
CE-B3LYP-B3LYP-D2/6-31G(d,p)				1.057	0.740	0.871	0.618			

surface, this interaction represents π–π interactions between the aromatic rings; the aryl and pyridine rings interact with an energy of −31.1 kJ mol^{-1}. The cocrystal network seems significantly influenced by other interactions, including those between DFPPI molecules that do not have π–π characteristics. Non-classical hydrogen-bond contacts like C(imine)—H···O(acid) and C(aryl)—H···O(carbonyl) also play a role in the interactions between the DFPPI and AcOH molecules. Finally, the rod-shaped energy frameworks (Fig. 5) highlight that the stability of the cocrystal is governed by multiple

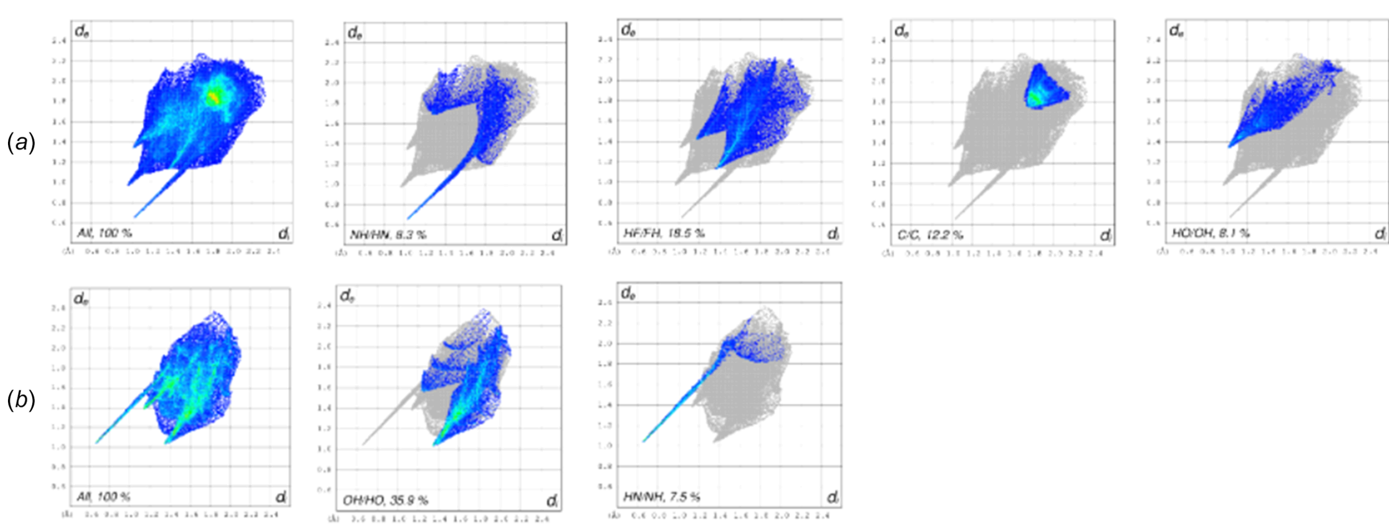

Figure 3
Selected 2D fingerprint plots for (*a*) (*E*)-*N*-(3,4-difluorophenyl)-1-(pyridin-4-yl)methanimine (*b*) and acetic acid in (**1**).

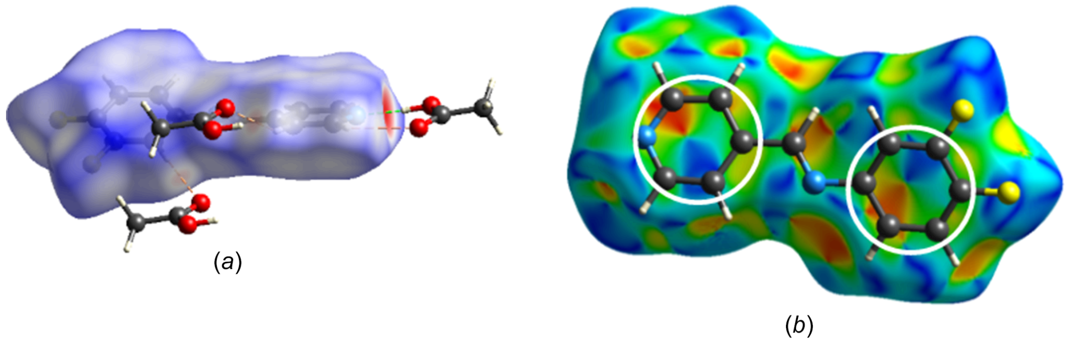

Figure 4
Hirshfeld surface mapped with (*a*) d_{norm}, with the hydrogen bonds between molecules, and (*b*) shape index. The red and blue triangles inside the rings agree with the presence of π–π interactions.

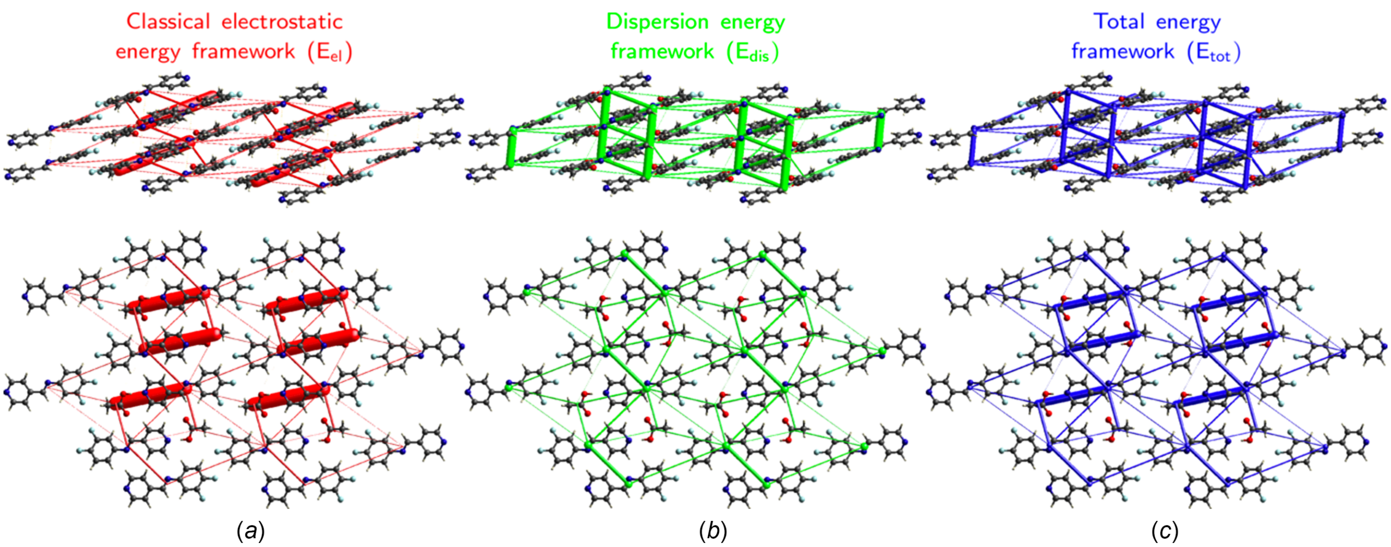

Figure 5
Perspective and top views of the energy frameworks of the cocrystal, showing the (*a*) electrostatic energy, (*b*) dispersion energy and (*c*) total energy. The radius of the cylinders is proportional to the relative strength of the corresponding energies. They were adjusted to the same scale factor of 80 with a cut-off value of 0 kJ mol^{-1} within a 2 × 2 × 2 unit cell.

electrostatic forces, with dispersive interactions having an important contribution, which is more significant between stacked molecules.

Theoretical electron-density analysis generates a spatial visualization and classifies pairwise interactions as attractive or repulsive (Fig. 6). Focusing on the four pairs with the most

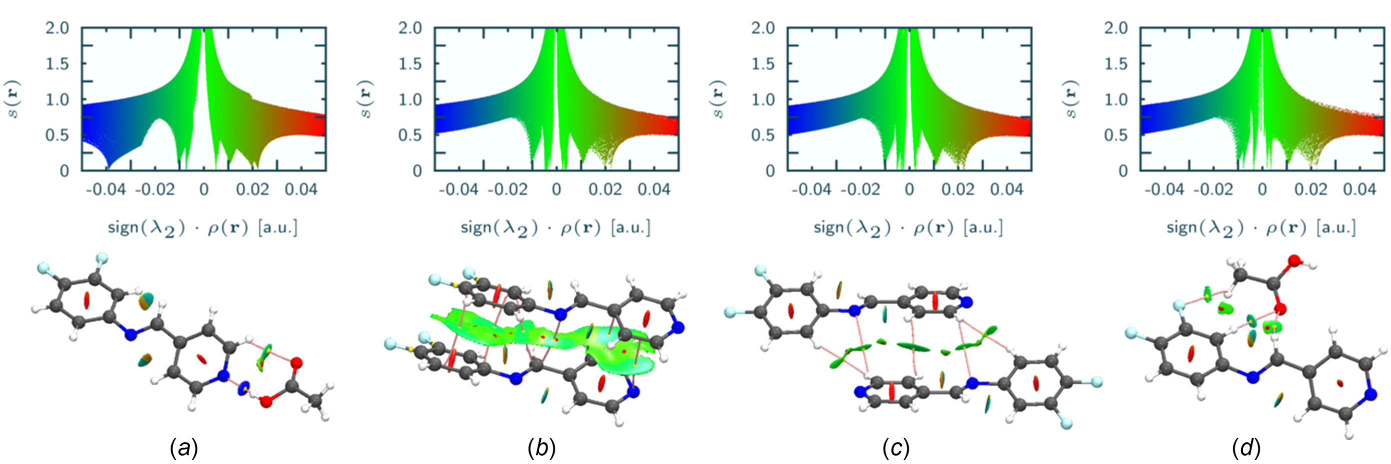

Figure 6
Plots of the reduced gradient of the density *s*(r) *versus* the electron density multiplied by the second Hessian eigenvalue (top) and molecular diagrams with the isosurfaces (isovalue = 0.5) of the *s*(r), the bond trajectories (pink) and the critical points (yellow) that exhibit the contacts for the dimers where the interactions were the strongest, based on the magnitude of E_{tot}. Parts (*a*)–(*d*) are for dimers corresponding to entries 1–4 of Table 4.

negative E_{tot} values, we observe bond trajectories for O—H···N and C—H···O hydrogen-bond contacts. Based on the NCI index, these interactions are attractive. Electrostatic interactions play a significant role in the total interaction energy of molecular pairs. Regarding stacking interactions, bonding trajectories connecting C atoms of interacting DFPPI molecules are identifiable, accompanied by a prominent isosurface indicative of weakly attractive stacking. Such characteristics align with the heightened dispersive character suggested by the E_{tot} components for these pairs.

Our assumption that a cocrystal would help study the intermolecular interactions of molecules that do not crystallize was successful. We found that having two F atoms in the aromatic ring is sufficient to promote π–π interactions between the aromatic rings, and further halogenation of the ^{F}Ar ring is unnecessary.

Funding information

Funding for this research was provided by: Dirección General de Asuntos del Personal Académico, Universidad Nacional Autónoma de México (grant No. PAPIIT: IN206722 to ADSP); Consejo Nacional de Humanidades Ciencia y Tecnología (scholarship to ADSP).

References

Aakeröy, C. B., Schultheiss, N., Desper, J. & Moore, C. (2007). *CrystEngComm*, **9**, 421–426.
Barbour, L. J. (2020). *J. Appl. Cryst.* **53**, 1141–1146.
Brammer, L. (2017). *Faraday Discuss.* **203**, 485–507.
Bruker (1998). *SAINT*. Bruker AXS Inc., Madison, Wisconsin, USA.
Bruker (2005). *APEX2*. Bruker AXS Inc., Madison, Wisconsin, USA.
Cruz, J. C., Hernández-Esparza, R., Vázquez-Mayagoitia, A., Vargas, R. & Garza, J. (2019). *J. Chem. Inf. Model.* **59**, 3120–3127.
Frisch, M. J., Trucks, G. W., Schlegel, H. B., Scuseria, G. E., Robb, M. A., Cheeseman, J. R., Scalmani, G., Barone, V., Petersson, G. A., Nakatsuji, H., Li, X., Caricato, M., Marenich, A. V., Bloino, J., Janesko, B. G., Gomperts, R., Mennucci, B., Hratchian, H. P., Ortiz, J. V., Izmaylov, A. F., Sonnenberg, J. L., Williams Ding, F., Lipparini, F., Egidi, F., Goings, J., Peng, B., Petrone, A., Henderson, T., Ranasinghe, D., Zakrzewski, V. G., Gao, J., Rega, N., Zheng, G., Liang, W., Hada, M., Ehara, M., Toyota, K., Fukuda, R., Hasegawa, J., Ishida, M., Nakajima, T., Honda, Y., Kitao, O., Nakai, H., Vreven, T., Throssell, K., Montgomery, J. A. Jr, Peralta, J. E., Ogliaro, F., Bearpark, M. J., Heyd, J. J., Brothers, E. N., Kudin, K. N., Staroverov, V. N., Keith, T. A., Kobayashi, R., Normand, J., Raghavachari, K., Rendell, A. P., Burant, J. C., Iyengar, S. S., Tomasi, J., Cossi, M., Millam, J. M., Klene, M., Adamo, C., Cammi, R., Ochterski, J. W., Martin, R. L., Morokuma, K., Farkas, O., Foresman, J. B. & Fox, D. J. (2016). *GAUSSIAN16*. Revision C.01. Gaussian Inc., Wallingford, CT, USA. https://gaussian.com/.
Galek, P. T. A., Chisholm, J. A., Pidcock, E. & Wood, P. A. (2014). *Acta Cryst.* B**70**, 91–105.
Groom, C. R., Bruno, I. J., Lightfoot, M. P. & Ward, S. C. (2016). *Acta Cryst.* B**72**, 171–179.
Gunawardana, C. A. & Aakeröy, C. B. (2018). *Chem. Commun.* **54**, 14047–14060.
Hernández-Esparza, R., Mejía–Chica, S., Zapata–Escobar, A. D., Guevara–García, A., Martínez–Melchor, A., Hernández–Pérez, J., Vargas, R. & Garza, J. (2014). *J. Comput. Chem.* **35**, 2272–2278.
Hernández-Esparza, R., Vázquez-Mayagoitia, A., Soriano-Agueda, L. A., Vargas, R. & Garza, J. (2018). *Int. J. Quantum Chem.* **119**, e25671.
Jaime-Adán, E., Hernández-Ortega, S., Toscano, R. A., Germán-Acacio, J. M., Sánchez-Pacheco, A. D., Hernández-Vergara, M., Barquera, J. E. & Valdés-Martínez, J. (2024). *Cryst. Growth Des.* **24**, 1888–1897.
Jayatilaka, D. & Grimwood, D. J. (2003). *Comput. Sci. ICCS*, pp. 142–151.
Lucassen, A. C. B., Vartanian, M., Leitus, G. & van der Boom, M. E. (2005). *Cryst. Growth Des.* **5**, 1671–1673.
Mackenzie, C. F., Spackman, P. R., Jayatilaka, D. & Spackman, M. A. (2017). *IUCrJ*, **4**, 575–587.
McKinnon, J. J., Jayatilaka, D. & Spackman, M. A. (2007). *Chem. Commun.* pp. 3814–3816.
McKinnon, J. J., Spackman, M. A. & Mitchell, A. S. (2004). *Acta Cryst.* B**60**, 627–668.
Mondal, B., Captain, B. & Ramamurthy, V. (2011). *Photochem. Photobiol. Sci.* **10**, 891–894.
Orbach, M., Choudhury, J., Lahav, M., Zenkina, O. V., Diskin-Posner, Y., Leitus, G., Iron, M. A. & van der Boom, M. E. (2012). *Organometallics*, **31**, 1271–1274.
Sánchez-Pacheco, A. D., Hernández-Vergara, M., Jaime-Adán, E., Hernández-Ortega, S. & Valdés-Martínez, J. (2021). *J. Mol. Struct.* **1234**, 130136.
Sheldrick, G. M. (2008). *Acta Cryst.* A**64**, 112–122.
Sheldrick, G. M. (2015*a*). *Acta Cryst.* A**71**, 3–8.
Sheldrick, G. M. (2015*b*). *Acta Cryst.* C**71**, 3–8.
Spackman, P. R., Turner, M. J., McKinnon, J. J., Wolff, S. K., Grimwood, D. J., Jayatilaka, D. & Spackman, M. A. (2021). *J. Appl. Cryst.* **54**, 1006–1011.
Spek, A. L. (2020). *Acta Cryst.* E**76**, 1–11.
Turner, M. J., Thomas, S. P., Shi, M. W., Jayatilaka, D. & Spackman, M. A. (2015). *Chem. Commun.* **51**, 3735–3738.

supporting information

Acta Cryst. (2024). C**80** [https://doi.org/10.1107/S2053229624005187]

Using cocrystals as a tool to study non-crystallizing molecules: crystal structure, Hirshfeld surface analysis and computational study of the 1:1 cocrystal of (*E*)-*N*-(3,4-difluorophenyl)-1-(pyridin-4-yl)methanimine and acetic acid

Addi Dana Sánchez-Pacheco, Eduardo H. Huerta, Josué Benjamín Espinosa-Camargo, Evelyn Valeria Rodríguez-Nájera, Diego Martínez-Otero, Simón Hernández-Ortega and Jesús Valdés-Martínez

Computing details

(*E*)-*N*-(3,4-difluorophenyl)-1-(pyridin-4-yl)methanimine; acetic acid

Crystal data

$C_{12}H_8F_2N_2 \cdot C_2H_4O_2$	$Z = 2$
$M_r = 278.26$	$F(000) = 288$
Triclinic, $P\overline{1}$	$D_x = 1.459$ Mg m^{-3}
$a = 3.8047$ (1) Å	Mo $K\alpha$ radiation, $\lambda = 0.71073$ Å
$b = 11.0101$ (4) Å	Cell parameters from 8212 reflections
$c = 15.4968$ (6) Å	$\theta = 2.5$–27.5°
$\alpha = 79.535$ (1)°	$\mu = 0.12$ mm^{-1}
$\beta = 89.223$ (1)°	$T = 100$ K
$\gamma = 82.880$ (1)°	Prism, colourless
$V = 633.42$ (4) Å^3	0.35 × 0.28 × 0.21 mm

Data collection

Bruker APEXII CCD diffractometer	2531 reflections with $I > 2\sigma(I)$
Radiation source: Incoatec ImuS	$R_{int} = 0.083$
ω scans	$\theta_{max} = 27.5°$, $\theta_{min} = 1.3°$
11642 measured reflections	$h = -4 \rightarrow 4$
2896 independent reflections	$k = -14 \rightarrow 14$
	$l = -20 \rightarrow 20$

Refinement

Refinement on F^2	Secondary atom site location: difference Fourier map
Least-squares matrix: full	Hydrogen site location: mixed
$R[F^2 > 2\sigma(F^2)] = 0.038$	H atoms treated by a mixture of independent and constrained refinement
$wR(F^2) = 0.110$	$w = 1/[\sigma^2(F_o^2) + (0.0586P)^2 + 0.0912P]$ where $P = (F_o^2 + 2F_c^2)/3$
$S = 1.06$	$(\Delta/\sigma)_{max} = 0.001$
2896 reflections	$\Delta\rho_{max} = 0.39$ e Å^{-3}
185 parameters	$\Delta\rho_{min} = -0.28$ e Å^{-3}
1 restraint	
Primary atom site location: structure-invariant direct methods	

Special details

Geometry. All esds (except the esd in the dihedral angle between two l.s. planes) are estimated using the full covariance matrix. The cell esds are taken into account individually in the estimation of esds in distances, angles and torsion angles; correlations between esds in cell parameters are only used when they are defined by crystal symmetry. An approximate (isotropic) treatment of cell esds is used for estimating esds involving l.s. planes.

Fractional atomic coordinates and isotropic or equivalent isotropic displacement parameters (Å²)

	x	y	z	U_{iso}*/U_{eq}
F1	1.2872 (2)	0.35402 (6)	0.05185 (4)	0.0267 (2)
F2	1.3162 (2)	0.14057 (7)	−0.00933 (4)	0.0270 (2)
O1	1.0367 (2)	0.26535 (7)	0.77019 (5)	0.0227 (2)
H1	1.149 (4)	0.2625 (16)	0.7221 (8)	0.034*
O2	0.9139 (2)	0.46992 (8)	0.71996 (5)	0.0248 (2)
N1	0.3443 (2)	0.25072 (9)	0.61506 (6)	0.0173 (2)
N2	0.8633 (2)	0.15059 (9)	0.33060 (6)	0.0160 (2)
C2	0.2908 (3)	0.35258 (10)	0.55249 (7)	0.0184 (2)
H2	0.170570	0.426595	0.567636	0.022*
C3	0.4024 (3)	0.35531 (10)	0.46656 (7)	0.0179 (2)
H3	0.356878	0.429362	0.423999	0.022*
C4	0.5820 (3)	0.24782 (10)	0.44380 (7)	0.0146 (2)
C5	0.6392 (3)	0.14168 (10)	0.50878 (7)	0.0165 (2)
H5	0.760800	0.066575	0.495690	0.020*
C6	0.5164 (3)	0.14717 (11)	0.59270 (7)	0.0186 (2)
H6	0.555773	0.074234	0.636467	0.022*
C7	0.7017 (3)	0.24845 (10)	0.35283 (7)	0.0162 (2)
H7	0.657799	0.322648	0.310346	0.019*
C8	0.9763 (3)	0.15414 (10)	0.24265 (7)	0.0150 (2)
C9	1.0735 (3)	0.26135 (10)	0.18881 (7)	0.0165 (2)
H9	1.062252	0.337691	0.209691	0.020*
C10	1.1855 (3)	0.25322 (11)	0.10491 (7)	0.0180 (2)
C11	1.2023 (3)	0.14296 (11)	0.07350 (7)	0.0188 (2)
C12	1.1089 (3)	0.03675 (11)	0.12571 (7)	0.0195 (2)
H12	1.118976	−0.038866	0.103919	0.023*
C13	0.9997 (3)	0.04275 (10)	0.21085 (7)	0.0175 (2)
H13	0.939981	−0.030190	0.248056	0.021*
C14	0.8935 (3)	0.37915 (10)	0.77688 (7)	0.0173 (2)
C15	0.7135 (3)	0.38455 (11)	0.86306 (8)	0.0218 (3)
H15A	0.891114	0.385338	0.908111	0.026*
H15B	0.587614	0.311498	0.879896	0.026*
H15C	0.544320	0.460336	0.857478	0.026*

Atomic displacement parameters (Å²)

	U^{11}	U^{22}	U^{33}	U^{12}	U^{13}	U^{23}
F1	0.0436 (5)	0.0192 (4)	0.0175 (3)	−0.0091 (3)	0.0047 (3)	−0.0008 (3)
F2	0.0417 (4)	0.0266 (4)	0.0145 (3)	−0.0054 (3)	0.0064 (3)	−0.0080 (3)
O1	0.0362 (5)	0.0146 (4)	0.0165 (4)	0.0001 (3)	0.0040 (3)	−0.0031 (3)

O2	0.0386 (5)	0.0161 (4)	0.0178 (4)	0.0005 (3)	0.0014 (4)	−0.0008 (3)
N1	0.0198 (5)	0.0170 (5)	0.0155 (4)	−0.0003 (4)	−0.0011 (4)	−0.0050 (4)
N2	0.0194 (5)	0.0146 (5)	0.0143 (4)	−0.0015 (3)	−0.0002 (4)	−0.0041 (3)
C2	0.0212 (6)	0.0139 (5)	0.0200 (5)	0.0026 (4)	−0.0003 (4)	−0.0063 (4)
C3	0.0219 (5)	0.0130 (5)	0.0176 (5)	0.0016 (4)	−0.0014 (4)	−0.0018 (4)
C4	0.0146 (5)	0.0146 (5)	0.0150 (5)	−0.0010 (4)	−0.0022 (4)	−0.0043 (4)
C5	0.0184 (5)	0.0117 (5)	0.0191 (5)	0.0019 (4)	−0.0007 (4)	−0.0045 (4)
C6	0.0221 (6)	0.0152 (5)	0.0171 (5)	0.0010 (4)	−0.0018 (4)	−0.0012 (4)
C7	0.0182 (5)	0.0147 (5)	0.0152 (5)	−0.0004 (4)	−0.0021 (4)	−0.0024 (4)
C8	0.0156 (5)	0.0150 (5)	0.0141 (5)	0.0012 (4)	−0.0020 (4)	−0.0039 (4)
C9	0.0201 (5)	0.0139 (5)	0.0157 (5)	0.0001 (4)	−0.0019 (4)	−0.0049 (4)
C10	0.0218 (5)	0.0159 (5)	0.0157 (5)	−0.0033 (4)	−0.0014 (4)	−0.0003 (4)
C11	0.0225 (6)	0.0223 (6)	0.0120 (5)	−0.0008 (4)	0.0002 (4)	−0.0058 (4)
C12	0.0243 (6)	0.0158 (5)	0.0197 (5)	−0.0011 (4)	−0.0007 (4)	−0.0079 (4)
C13	0.0208 (5)	0.0138 (5)	0.0180 (5)	−0.0020 (4)	−0.0003 (4)	−0.0034 (4)
C14	0.0204 (5)	0.0163 (5)	0.0161 (5)	−0.0019 (4)	−0.0032 (4)	−0.0050 (4)
C15	0.0262 (6)	0.0220 (6)	0.0179 (5)	−0.0028 (5)	0.0026 (5)	−0.0059 (4)

Geometric parameters (Å, º)

F1—C10	1.3504 (13)	C5—H5	0.9500
F2—C11	1.3531 (12)	C6—H6	0.9500
O1—C14	1.3243 (14)	C7—H7	0.9500
O1—H1	0.858 (9)	C8—C13	1.3951 (16)
O2—C14	1.2166 (14)	C8—C9	1.4029 (15)
N1—C2	1.3391 (14)	C9—C10	1.3777 (15)
N1—C6	1.3419 (15)	C9—H9	0.9500
N2—C7	1.2739 (15)	C10—C11	1.3818 (17)
N2—C8	1.4188 (13)	C11—C12	1.3783 (16)
C2—C3	1.3884 (15)	C12—C13	1.3884 (15)
C2—H2	0.9500	C12—H12	0.9500
C3—C4	1.3917 (15)	C13—H13	0.9500
C3—H3	0.9500	C14—C15	1.5000 (15)
C4—C5	1.3938 (15)	C15—H15A	0.9800
C4—C7	1.4746 (14)	C15—H15B	0.9800
C5—C6	1.3850 (15)	C15—H15C	0.9800
C14—O1—H1	113.1 (11)	C10—C9—C8	118.37 (10)
C2—N1—C6	117.64 (9)	C10—C9—H9	120.8
C7—N2—C8	119.44 (9)	C8—C9—H9	120.8
N1—C2—C3	123.21 (10)	F1—C10—C9	119.95 (10)
N1—C2—H2	118.4	F1—C10—C11	118.55 (10)
C3—C2—H2	118.4	C9—C10—C11	121.49 (10)
C2—C3—C4	118.93 (10)	F2—C11—C12	120.40 (10)
C2—C3—H3	120.5	F2—C11—C10	118.78 (10)
C4—C3—H3	120.5	C12—C11—C10	120.81 (10)
C3—C4—C5	118.06 (10)	C11—C12—C13	118.52 (10)
C3—C4—C7	119.85 (10)	C11—C12—H12	120.7

C5—C4—C7	122.09 (10)	C13—C12—H12	120.7
C6—C5—C4	119.10 (10)	C12—C13—C8	121.07 (10)
C6—C5—H5	120.4	C12—C13—H13	119.5
C4—C5—H5	120.4	C8—C13—H13	119.5
N1—C6—C5	123.06 (10)	O2—C14—O1	123.43 (10)
N1—C6—H6	118.5	O2—C14—C15	123.74 (10)
C5—C6—H6	118.5	O1—C14—C15	112.80 (9)
N2—C7—C4	120.72 (10)	C14—C15—H15A	109.5
N2—C7—H7	119.6	C14—C15—H15B	109.5
C4—C7—H7	119.6	H15A—C15—H15B	109.5
C13—C8—C9	119.71 (10)	C14—C15—H15C	109.5
C13—C8—N2	116.81 (10)	H15A—C15—H15C	109.5
C9—C8—N2	123.45 (10)	H15B—C15—H15C	109.5

C6—N1—C2—C3	0.39 (17)	C13—C8—C9—C10	0.87 (16)
N1—C2—C3—C4	−0.65 (17)	N2—C8—C9—C10	178.78 (10)
C2—C3—C4—C5	0.43 (16)	C8—C9—C10—F1	−178.78 (10)
C2—C3—C4—C7	179.76 (10)	C8—C9—C10—C11	0.20 (17)
C3—C4—C5—C6	0.00 (16)	F1—C10—C11—F2	−0.67 (17)
C7—C4—C5—C6	−179.31 (10)	C9—C10—C11—F2	−179.67 (10)
C2—N1—C6—C5	0.08 (17)	F1—C10—C11—C12	178.57 (10)
C4—C5—C6—N1	−0.27 (17)	C9—C10—C11—C12	−0.43 (18)
C8—N2—C7—C4	−179.80 (9)	F2—C11—C12—C13	178.80 (10)
C3—C4—C7—N2	−179.29 (10)	C10—C11—C12—C13	−0.42 (18)
C5—C4—C7—N2	0.01 (17)	C11—C12—C13—C8	1.50 (17)
C7—N2—C8—C13	−151.63 (11)	C9—C8—C13—C12	−1.74 (17)
C7—N2—C8—C9	30.40 (16)	N2—C8—C13—C12	−179.79 (10)

Hydrogen-bond geometry (Å, º)

D—H···*A*	*D*—H	H···*A*	*D*···*A*	*D*—H···*A*
O1—H1···N1^{i}	0.86 (1)	1.83 (1)	2.6819 (12)	174 (2)
C2—H2···O2^{ii}	0.95	2.64	3.3344 (14)	130
C3—H3···O2^{iii}	0.95	2.48	3.3174 (14)	147
C9—H9···O2^{iv}	0.95	2.56	3.5088 (14)	173
C13—H13···O1^{v}	0.95	2.65	3.3713 (14)	134
C15—H15*B*···F2^{vi}	0.98	2.61	3.5224 (14)	155

Symmetry codes: (i) *x*+1, *y*, *z*; (ii) *x*−1, *y*, *z*; (iii) −*x*+1, −*y*+1, −*z*+1; (iv) −*x*+2, −*y*+1, −*z*+1; (v) −*x*+2, −*y*, −*z*+1; (vi) *x*−1, *y*, *z*+1.